PROCEEDINGS of the
23rd International Congress on Acoustics
9 to 13 September 2019 in Aachen, Germany

An immersed boundary method for fluid–structure–acoustics interaction at low Reynolds numbers

Li Wang[(1)], Fang-bao Tian[(2)], Joseph C. S. Lai[(3)]

[(1)]School of Engineering and Information Technology, University of New South Wales, Canberra ACT, 2600, Australia, l.wang@unsw.edu.au

[(2)]School of Engineering and Information Technology, University of New South Wales, Canberra ACT, 2600, Australia, f.tian@adfa.edu.au

[(3)]School of Engineering and Information Technology, University of New South Wales, Canberra ACT, 2600, Australia, j.lai@adfa.edu.au

Abstract

This paper presents an immersed boundary method for fluid–structure–acoustics interactions involving complex boundaries at low Reynolds numbers. In this method, the compressible Navier–Stokes equations are considered, where a fifth-order accuracy Weighted Essentially Non-Oscillation (WENO) scheme and a fourth-order central difference scheme are adopted to discretize the convective and diffusion terms, respectively. The third-order Runge-Kutta method is used for the temporal discretization. The non-linear flexible structure immersed in the fluid is numerically solved by using a finite element method. By using a penalty immersed boundary method, the no-slip boundary between the fluid and the structure is achieved. Acoustic waves scattering benchmark problems and sound generation by a micro flapping vehicle are presented to validate the present solver. Comparisons with the published data are presented to demonstrate the good performance of the present method in modelling acoustics. The capability of using this method to study the sound generation by flapping plates is also demonstrated.

Keywords: Fluid–structure interaction, Immersed boundary method, Large deformation, Acoustics

1 INTRODUCTION

Flow-induced sound extensively exists in engineering applications, such as aviation technologies [1], ventilation [2] and biomechanics [3]. Direct numerical simulation that solves the compressible Navier-Stokes equations is an effective method for computational aeroacoustics (CAA). In the traditional computatiaonl fluid dynamics (CFD), conformal mesh is generally used [4], which is time consuming especially when handling fluid–structure interaction (FSI) problems involving large deformations. The immersed boundary (IB) method developed by Peskin [5] has proven to be an efficient method for this type of FSI simulations. By using this method, the conformal mesh is not needed and the regeneration of mesh is also avoided. Because of its simple boundary treatment, IB method has gained popularity for a wide range of applications [6, 7]. Penalty IB (pIB) is a typical IB method [8] where the IB is conceptually split into two Lagrangian components: one component is massless and interacts with the fluid exactly as the traditional IB method, and the other component carrying mass is connected to the massless component by virtual stiff springs. However, most of the previous studies based on IB method focus on FSI problems without acoustics [9, 10, 11, 12]. Sun et al. presented an IB method which considers the linear Euler equations for acoustic scattering modeling [13], but the viscosity of the fluid is not considered.

Here, an immersed boundary method for fluid–structure–acoustics interactions involving complex boundaries at low Reynolds numbers are presented. The organization of the paper is as follows. The numerical approach is briefly introduced in Section 2. Two validations including acoustic waves scattered by a stationary cylinder and sound generation by a micro flapping vehicle are presented in Section 3. The final conclusions are given in

Section 4.

2 NUMERICAL METHOD

In this section, the in-house solver used will be introduced briefly, and the details can be found in our previous work [12, 14]. In this method, the compressible fluid flow, structural dynamics and fluid–structure interaction between them are considered. The structure is assumed to be elastic and its dynamics is governed by the following non-linear equation

$$\rho_s \frac{\partial X}{\partial t} + \frac{\partial}{\partial s}\left[(K_S|\frac{\partial X}{\partial s}| - 1)\frac{\partial X}{\partial s}\right] + K_B \frac{\partial X^4}{\partial s^4} = F_f, \tag{1}$$

where X is the Lagrangian coordinates of the flexible beam, ρ_s is linear density, K_S and K_B are respectively the stretching and bending rigidity, s is the arc coordinate, and F_f is the external force acting on the beam. Absolute nodal coordinates formulation proposed by Shabana [15] is adopted in the structure solver to solve Eq. (1).

The flow dynamics is governed by the two-dimensional compressible viscous Navier–Stokes equations

$$\frac{\partial Q}{\partial t} + \frac{\partial F}{\partial x} + \frac{\partial G}{\partial y} + \frac{1}{Re}(\frac{\partial F_u}{\partial x} + \frac{\partial G_v}{\partial y}) = S, \tag{2}$$

where $Q = [\rho, \rho u, \rho v, E]^T$, $F = [\rho u, \rho u^2 + P, \rho uv, (E+P)u]^T$, $G = [\rho v, \rho uv, \rho v^2 + P, (E+P)v]^T$, $F_u = [0, \tau_{xx}, \tau_{xy}, b_x]^T$, $G_v = [0, \tau_{xy}, \tau_{yy}, b_y]^T$, $b_x = u\tau_{xx} + v\tau_{xy}$,$b_y = u\tau_{xy} + v\tau_{yy}$. ρ is the fluid density, u, v and w are respectively the three velocity components, P is the pressure, E is the total energy, S is a general source term including the IB-imposed Eulerian force and other body forces, Re is the Reynolds number, and τ_{ij} is the shear stress.

In the fluid solver, the fifth-order accuracy WENO scheme proposed by Liu et al. [16] is employed for the spatial discretization of the convective term. For the viscous term, a fourth-order central difference scheme is used to discretize the spatial derivatives. For all unsteady equations in the flow solver, the third-order TVD Runge-Kutta method is used for time discretization. The dynamics of the fluid and flexible structures are solved independently and the interaction force is calculated explicitly using a feedback law based on the pIB method.

3 VALIDATIONS AND APPLICATIONS

3.1 Acoustics wave scattered by a stationary cylinder

In order to verify the accuracy of the method in simulating the acoustic problem, acoustic wave scattered from a stationary cylinder is validated against the published data [17]. In this problem, a rigid cylinder with a diameter of $D = 1.0$ is fixed with its center at (0, 0). The initial conditions are localized perturbations of the Gaussian distribution of pressure P,

$$P = \varepsilon \exp[-\ln(2)\frac{(x-4)^2 + y^2}{0.04}] \tag{3}$$

where $\varepsilon = 10^{-3}$. The initial density and pressure are respectively 1.0 and $1/\gamma$ (the adiabatic coefficient $\gamma = 1.4$), and the initial velocity of the fluid is zero.

We used a uniform Cartesian mesh over a computational domain of $(16D \times 12D)$ with three different mesh spacings: $D/100$, $D/50$ and $D/25$. The time histories of the fluctuation pressure, $\Delta p = P - p_0$ where P and p_0 are respectively the current and initial pressure, from a numerical probe located at (2, 0) are plotted in Fig. 1 along with the exact results reported in Ref. [17]. According to the comparisons in Fig. 1, all the three mesh spacings can well capture the fluctuating pressure, and the small discrepancies depicted in the scaled up figures can be diminished when the mesh size is $D/100$.

Comparison of Δp contours obtained by Bailoor et al. [18] and this study at the time of 6.0 in Fig. 2 shows that the collision, merge and reflection of the acoustic waves are well captured by our numerical method.

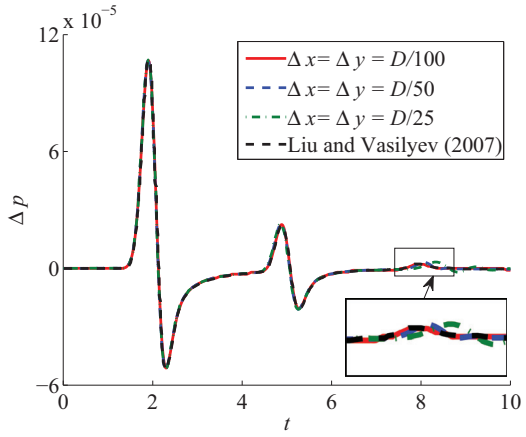

Figure 1. Time histories of the fluctuating pressure measured at (2,0).

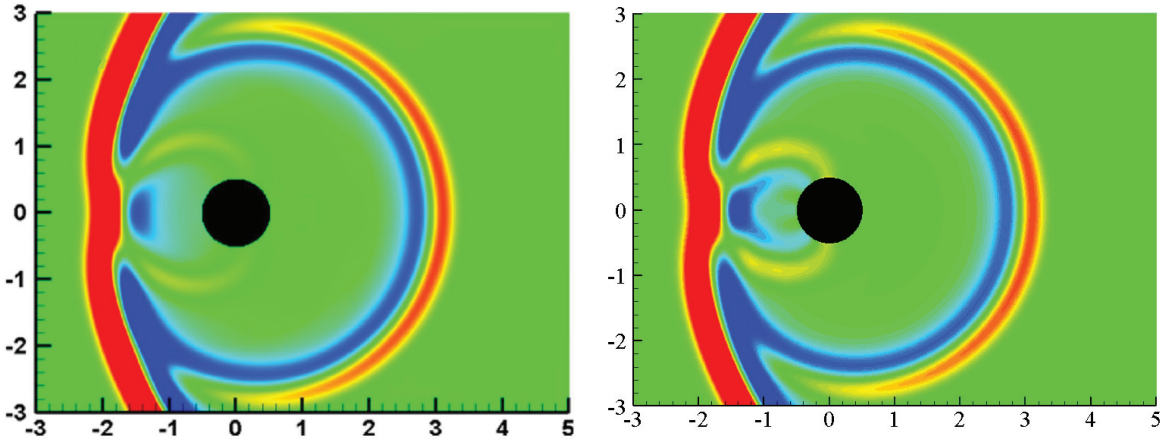

Figure 2. Fluctuating pressure at $t = 6$ obtained by Bailoor et al. [18] (left) and the present simulation (right). The contour level ranges from -2.0×10^{-5} to 2.0×10^{-5}.

3.2 Sound generation by a micro flapping vehicle

Here, a micro flapping vehicle in hovering flight is considered to validate the current solver in handling moving body with relatively complex geometry configuration. The schematic of the problem is shown in Fig. 3. A circular cylinder (body) with a diameter of $0.5L$, and two elliptic cylinders (wings) with the dimensions of L and $0.4L$ are used to model the micro flapping vehicle. The two wings flap symmetrically, and the flapping motion of the wings is prescribed by

$$\alpha(t) = \alpha_0[1 + sin(2\pi ft)], \tag{4}$$

where the amplitude of the flapping angle α_0 is 25.3^o and f is the flapping frequency. The Reynolds number defined by $\rho_f U_{max} L/\mu$ is 200, where U_{max} is the maximum wing tip velocity. The Strouhal number defined by fL/U_{max} is 0.25, and the Mach number based on U_{max} is 0.1. The computational domain extends from $(-100L, -100L)$ to $(100L, 100L)$, with 50 points to resolve the wing length.

A direct comparison of the lifts generated by the body and wing is shown in Fig. 4. It is found that these results

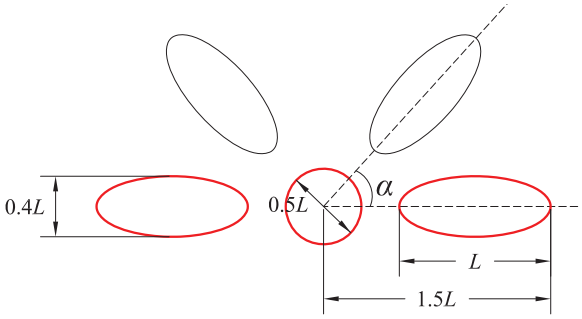

Figure 3. Schematic of the prescribed flapping motion of a micro flapping vehicle.

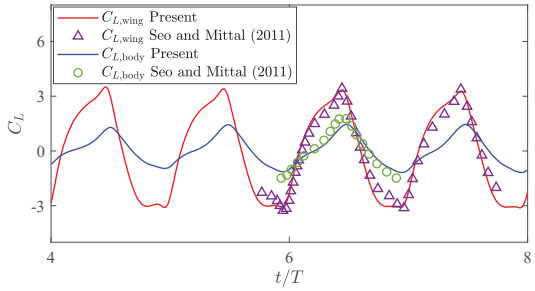

Figure 4. Sound generation by a micro flapping vehicle in hovering flight: comparison of the lift generated by the wing and body.

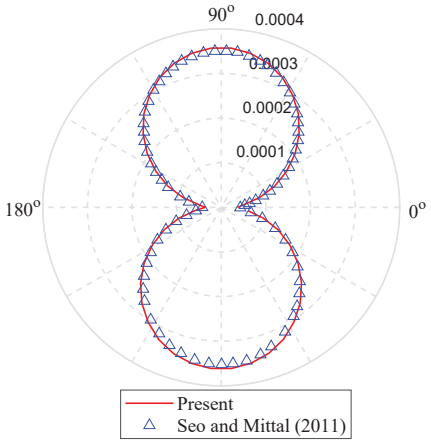

Figure 5. Sound generation by a micro flapping vehicle in hovering flight: comparison of the root-mean-square of fluctuating pressure measured at a distance of 50L.

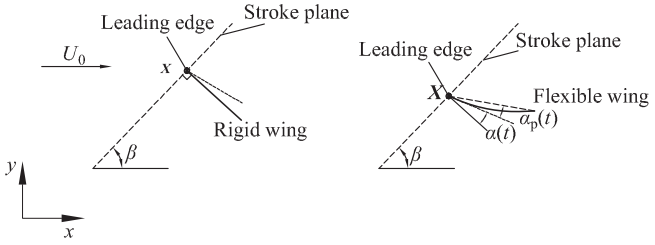

Figure 6. Schematic of a rigid (left) and flexible (right) foil flapping in a uniform flow.

agree well with the data from Ref. [19]. The fluctuating pressure $\Delta\tilde{p}$ is defined by $\Delta\tilde{p}(x,y,t) = \Delta p(x,y,t) - \Delta\bar{p}(x,y)$, where Δp denotes the total fluctuating pressure and $\bar{p}$ is the time average pressure. $\Delta p = p - p_\infty$ with p_∞ being the ambient pressure. Good agreements of the root-mean-square of fluctuating pressure measured at a distance of $50L$ shown in Fig. 5 confirm the good performance of the current method in handling acoustics involving complex moving geometries.

3.3 Sound generation by a flexible flapping plate

Here, the acoustic perturbations induced by flapping foils in forward flight are considered, as shown in Fig. 6 [20]. The foil is clamped at the leading edge, and the clamping device undergoes a combined translational and rotational motions, given by [20]

$$\begin{aligned} X_0(t) &= \frac{A_0}{2}\cos(2\pi ft)[\cos\beta, \sin\beta], \\ \alpha(t) &= \frac{\alpha_m}{2}\sin(2\pi ft + \phi). \end{aligned} \tag{5}$$

where A_0 is the translational amplitude, f is the flapping frequency, α_m is the rotation amplitude, and β is the angle between the stroke plane and the horizontal plane. The phase difference (ϕ) is 0.

The non-dimensional parameters including the flapping amplitude, Reynolds number, inlet velocity, Mach number, mass ratio and frequency ratio that control this problem are given respectively by

$$\frac{A_0}{L}, \quad \mathrm{Re} = \frac{\rho_f U L}{\mu}, \quad U_r = \frac{U_0}{U}, \quad M = \frac{\pi U}{2c}, \quad m^* = \frac{\rho_s}{\rho_f L}, \quad \omega^* = \frac{2\pi f}{\omega_n}, \tag{6}$$

where L is the chord length, $U = 2fA_0$ is the average translational velocity of the leading edge, f is the flapping frequency of the foil, c is the sound speed of the fluid, ρ_f is the fluid density, ρ_s is the linear density of the foil, and $\omega_n = k_n^2/L^2\sqrt{E_B/\rho_s}$ with $k_n = 1.8751$ (the frequency of the first natural vibration mode of the wing with fixed leading edge) and E_B being the bending rigidity. Here, Re=100, $m* = 5.0$ and $U_r = 0.4$. The thrust, lift and power coefficients are defined as

$$C_T = \frac{2F_T}{\rho_f U^2 L}, \quad C_L = \frac{2F_L}{\rho_f U^2 L}, \quad C_p = \frac{-2\int_0^L F_f \cdot v dl}{\rho_f U^3 L}, \tag{7}$$

where F_T and F_L are respectively the thrust and lift force acting on the foil by the ambient fluid, F_f is the hydrodynamic traction on the foil, and v is the velocity of the foil. The fluctuating pressure $\Delta\tilde{p}$ is defined in the same way in Section 3.2. All the pressures presented afterwards are scaled by the fluid density ρ_f and sound speed c.

In order to compare the sound generation of rigid and flexible foils, the polar diagrams of the root-mean-square of $\Delta\tilde{p}$ measured at $r = 30L$ are presented in Fig. 7. As shown in Fig. 7 (a) and (c), $\Delta\tilde{p}$ generated by the rigid plate and NACA0015 foil distributes symmetrically about the stroke plane (indicated by the dashed line

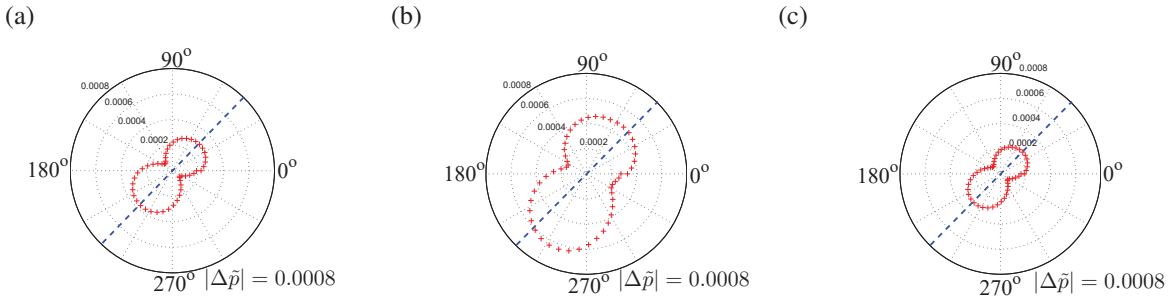

Figure 7. Flapping foils in forward flight: root-mean-square of $\Delta\tilde{p}$ measured at $r = 30L$: (a) rigid plate, (b) flexible plate and (c) NACA0015 foil. Re=100, $M = 0.1$, $Ur = 0.4$, $A_0/L = 1.25$ and $\alpha_m = \pi/4$. The dashed lines indicate the directions of the stroke planes.

in Fig. 7 (a) and (c)). However, Fig. 7 (b) shows that the distribution of the fluctuating pressure generated by the flexible foil is asymmetrical. An evident shift (about 15^o anticlockwise) is observed, as shown in Fig. 7 (b). As analyzed in Ref. [20], the deformation of the flexible plate during upstroke is higher than that during downstroke, due to the presence of free stream. Obviously, this sound shift is introduced by the asymmetrical deformation of the foil. Fig. 7 also shows that the flexible plate generates the largest fluctuating pressure, which is significantly larger (up to 50%) than that generated by the rigid plate and NACA0015 foil. The results indicate that the flexibility influences the sound generation significantly. The effects of geometrical shape on the sound amplitudes are much smaller. In addition, it is found that the fluctuating pressure on the lower section is larger than that on the upper section. A reasonable explanation is that the lower section is located on the windward side and the upper section is on the leeward side.

4 CONCLUSIONS

An immersed boundary method for fluid–structure–acoustics interactions involving complex boundaries at low Reynolds numbers is presented. In this method, the compressible Navier–Stokes equations and the non-linear flexible structure immersed in the fluid are numerically solved by using a finite difference method and a finite element method, respectively. By using a penalty immersed boundary method, the no-slip boundary between the fluid and the structure is achieved. Comparisons with the published data indicate the good performance of this method in modelling acoustics for acoustic waves scattering by a rigid cylinder and the sound generation by a micro flapping vehicle. The capability of this method to study the sound generation by flapping plates is also demonstrated.

ACKNOWLEDGEMENTS

Dr. F.-B. Tian is the recipient of an Australian Research Council Discovery Early Career Researcher Award (project number DE160101098). This work was conducted with the assistance of resources from the National Computational Infrastructure (NCI), which is supported by the Australian Government.

REFERENCES

[1] Colonius, Tim and Lele, Sanjiva K, 2004. “Computational aeroacoustics: progress on nonlinear problems of sound generation”. *Progress in Aerospace Sciences,* ***40(6)***, pp. 345–416.

[2] Waye, K.P., Rylander, R., Benton, S. and Leventhall, H.G., 1997. "Effects on performance and work quality due to low frequency ventilation noise". *Journal of Sound and Vibration,* ***205(4)***, pp. 467–474.

[3] Seo, Jung Hee and Mittal, Rajat, 2011. "A high-order immersed boundary method for acoustic wave scattering and low-Mach number flow-induced sound in complex geometries". *Journal of Computational Physics,* ***230(4)***, pp. 1000–1019.

[4] Tian, F.B., Bharti, R.P. and Xu, Y.Q., 2014. "Deforming-Spatial-Domain/Stabilized Space–Time (DSD/SST) method in computation of non-Newtonian fluid flow and heat transfer with moving boundaries". *Computational Mechanics,* ***53(2)***, pp. 257–271.

[5] Peskin, C.S., 1977. "Numerical analysis of blood flow in the heart". *Journal of Computational Physics,* ***25(3)***, pp. 220–252.

[6] Tian, F.B., Dai, H., Luo, H., Doyle, J.F. and Rousseau, B., 2014. "Fluid–structure interaction involving large deformations: 3D simulations and applications to biological systems". *Journal of Computational Physics,* ***258***, pp. 451–469.

[7] Huang, W.X., Shin, S.J. and Sung, H.J., 2007. "Simulation of flexible filaments in a uniform flow by the immersed boundary method". *Journal of Computational Physics,* ***226(2)***, pp. 2206–2228.

[8] Kim, Y. and Peskin, C.S., 2007. "Penalty immersed boundary method for an elastic boundary with mass". *Physics of Fluids,* ***19(5)***, p. 053103.

[9] Mittal, R. and Iaccarino, G., 2005. "Immersed boundary methods". *Annu. Rev. Fluid Mech.,* ***37***, pp. 239–261.

[10] Tian, Fang-Bao and Luo, Haoxiang and Zhu, Luoding and Liao, James C and Lu, Xi-Yun, 2011. "An efficient immersed boundary-lattice Boltzmann method for the hydrodynamic interaction of elastic filaments". *Journal of Computational Physics,* ***230(19)***, pp. 7266–7283.

[11] Ghias, Reza and Mittal, Rajat and Dong, Haibo, 2007. "A sharp interface immersed boundary method for compressible viscous flows". *Journal of Computational Physics,* ***225(1)***, pp. 528–553.

[12] Wang, L., Currao, G.M., Han, F., Neely, A.J., Young, J. and Tian, F.B., 2017. "An immersed boundary method for fluid–structure interaction with compressible multiphase flows". *Journal of Computational Physics,* ***346***, pp. 131–151.

[13] Sun, Xiaofeng and Jiang, Yongsong and Liang, An and Jing, Xiaodong, 2012. "An immersed boundary computational model for acoustic scattering problems with complex geometries". *The Journal of the Acoustical Society of America,* ***132(5)***, pp. 3190–3199.

[14] Wang, Li and Tian, Fang-Bao and Lai, Joseph CS, 2019. "An immersed boundary method for fluid–structure–acoustics interactions involving large deformations and complex geometries". *Under review*.

[15] Shabana, A.A., 1997. "Flexible multibody dynamics: review of past and recent developments". *Multibody System Dynamics,* ***1(2)***, pp. 189–222.

[16] Liu, Xu-Dong and Osher, Stanley and Chan, Tony, 1994. "Weighted essentially non-oscillatory schemes". *Journal of Computational Physics,* ***115(1)***, pp. 200–212.

[17] Liu, Q. and Vasilyev, O.V., 2007. "A Brinkman penalization method for compressible flows in complex geometries". *Journal of Computational Physics,* ***227(2)***, pp. 946–966.

[18] Bailoor, S., Annangi, A., Seo, J.H. and Bhardwaj, R., 2017. "Fluid–structure interaction solver for compressible flows with applications to blast loading on thin elastic structures". *Applied Mathematical Modelling,* ***52***, pp. 470–492.

[19] Seo, Jung-Hee and Mittal, Rajat, 2011. "Computation of aerodynamic sound around complex stationary and moving bodies". *49th AIAA Aerospace Sciences Meeting including the New Horizons Forum and Aerospace Exposition*, pp. 1087.

[20] Tian, Fang-Bao and Luo, Haoxiang and Song, Jialei and Lu, Xi-Yun, 2013. "Force production and asymmetric deformation of a flexible flapping wing in forward flight". *Journal of Fluids and Structures,* ***36***, pp. 149–161.